Spectral response of the photoconductance: a new technique for solar cell characterization

H. Mäckel and A. Cuevas
Centre of Sustainable Energy Systems, Faculty of Engineering and Information Technology
Australian National University, Canberra, ACT
AUSTRALIA
E-mail: mackel@faceng.anu.edu.au

W. Warta
Fraunhofer Institut für Solare Energiesysteme
Heidenhofstraße 2, 79110 Freiburg
GERMANY

A new technique, the spectral response of the steady-state photoconductance, is proposed for solar cell characterization in research and development. The method is experimentally demonstrated with solar cell precursors having emitters with markedly different levels of surface and bulk recombination losses. A high-efficiency solar cell has been investigated, comparing the new spectral response method to the conventional spectral response. The spectral response of the photoconductance has been measured with a contactless quasi-steady state photoconductance method (QSSPC) using light of different wavelengths. The measured spectral response of the photoconductance has been compared to PC1D simulations. A good agreement between theory and experiment, and between the two spectral response techniques has been found. The main advantages of the spectral photoconductance technique are that it is fast, contactless, and can be used immediately after junction formation before metallization. These properties make it very appropriate for routine monitoring of the emitter region, including in-line process control.

1. INTRODUCTION

The spectral response, that is, the ratio of short-circuit current density and incident illumination power as functions of wavelength, is a powerful tool for the development and calibration of solar cells. It is commonly used to characterize the ability to collect charge carriers generated by different wavelengths of the sun spectrum. As light of different colors is absorbed at differently depths in the solar cell, the spectral response provides a depth resolution of the recombination processes, which hinder charge carriers to be collected. The spectral response is therefore particularly useful to optimize the emitter region whose dopant density profile has to be carefully adjusted between the compromise of a high short-circuit current and low series resistance. The measurement of the spectral response requires finished solar cells to be able to extract short-circuit current. In this paper we propose a new measurement method, the spectral response of the quasi-steady-state photoconductance, briefly QSSPC-λ, with the advantage that it can be used throughout the solar cell fabrication.

The photoconductance technique has been widely used in the past to reveal recombination parameters such as charge carrier lifetime and surface recombination velocity. The quasi-steady-state photoconductance (QSSPC) has become increasingly popular [1], because it yields information on the actual recombination parameters and injection dependencies are analysed with a single measurement. In comparison, a single measurement performed with the microwave-detected photoconductance decay (MW-PCD) method only deduced differential recombination parameters at one injection level [2]. The usefulness of the spectral response of the photoconductance has been demonstrated in recent works. A two-wavelength method has been proposed to separate bulk and surface recombination in non-passivated silicon wafers [3] and to extract quantum efficiencies of the emitter region [4,5]. The spectral photoconductance has also been used to characterize light trapping in silicon films [6].

The two-wavelength method consists in the illumination of the wafer at two wavelengths in the UV and in the IR. The UV light is absorbed near the surface while illumination with infrared light is absorbed deep in the wafer. In the case of a non-passivated silicon wafer, the UV light favours surface recombination whereas the IR light emphasizes bulk recombination. By solving the minority carrier diffusion equation for the two wavelengths, the remaining unknown parameters, the surface recombination velocity and the bulk lifetime, can be derived [3]. When

we consider a silicon sample with emitter region, the illumination of UV light favours beside the surface recombination also recombination within the emitter. Cuevas *et al*. observed that the spectral response of the photoconductance behaves similarly to the spectral response of short-circuit current [5]. Thus, the spectral response of the photoconductance for UV is strongly dependent on the emitter quantum collection efficiency. On the other hand, the latter has very little impact on the photoconductance for longer wavelength light, and this provides a basis for comparison. By taking the ratio of the photoconductance response at UV and IR light, an emitter quantum efficiency of the photoconductance can be defined. Cuevas *et al*. have demonstrated the usefulness of this parameter for different emitter profiles and passivation schemes [5]. As quasi-steady-state photoconductance measurements are contactless, the method can be applied directly after emitter diffusion.

Cuevas et al have compared the traditional spectral response of short-circuit current to the response of the open-circuit photoconductance using the computer program PC1D [5]. In the case of a passivated emitter used for high-efficiency solar cells the shapes of the spectral response of the short-circuit current and the photoconductance are identical. If the emitter is non-passivated, the traditional and the photoconductance response agree well in the 400-800 nm range and diverge in the IR emitters [5]. Photogeneration near the front surface results in a lower photoconductance due to the high surface recombination than photogeneration deep in the wafer [3]. The high recombination can become a diffusion limit for charge carrier generated deep in the wafer to be collected at the front surface. The enhanced IR response is therefore not seen in the spectral response of short-circuit current. The examples show that for passivated high-efficiency emitter structures the QSSPC-λ method is an alternative way to describe the spectral response of solar cells for all wavelengths of the sun spectrum. In the case of non-passivated high-efficiency emitters, the method is valid in the range 400-800 nm. This paper demonstrates the validation of the QSSPC-λ method for high-efficiency silicon solar cell devices expanding the two-wavelength method to all wavelengths of the sun spectrum.

2. SPECTRAL RESPONSE OF A SOLAR CELL

The physical difference between the conventional spectral response and the spectral response of the photoconductance should be clearly outlined: In the first case, the current density is measured in short-circuit conditions, that means, no voltage is applied between the contacts. In contrast, the photoconductance measurement is a contactless method, which signifies that no charge carriers are withdrawn off the device. This leads to different boundary conditions at the front and back surfaces and further to a different minority carrier density throughout the device. To distinguish between the two methods, the parameters have been labelled either with the suffix "*sc*" or "*oc*".

The conventional spectral response is defined as the dependence of the collected charge carriers on the incident photons of different wavelengths, λ. In general, the spectral response is normalized to its maximum possible value, that is, the ideal spectral response $SR_{ideal} = \lambda$ (nm)/(1240 eVnm/C), where λ is the wavelength of illumination expressed in nm and the factor 1240 is the wavelength in vacuum of a 1eV photon. The normalized spectral response, the external quantum efficiency, *EQE*, is given by the ratio of the short-circuit current density, J_{sc}, to the incident photon flux on the surface of the solar cell, N_{ph}:

$$EQE(J_{sc}) = \frac{J_{sc}(\lambda)}{qN_{ph}(\lambda)} \tag{1}$$

The external quantum efficiency can also be described by the optical and electronic mechanisms that determine it. The *EQE* can be separated into the optical part: the fraction of incident photons that are absorbed in the sample, f_{abs}, and the electrical part: the probability that the carriers generated by those photons are collected at the p-n junction, η_c^{sc}:

$$EQE(J_{sc}) = f_{abs} \cdot \eta_c^{sc} \tag{2}$$

Similar to the definition in equation (1), the external quantum efficiency of the open-circuit photoconductance $EQE(\sigma_{oc})$ is defined as the ratio of the photoconductance and the incident number of photons:

$$EQE(\sigma_{oc}) = \frac{\sigma_{oc}(\lambda)}{qN_{ph}(\lambda)} \tag{3}$$

The photoconductance is very sensitive to surface recombination and strongly lowers $EQE(\sigma_{oc})$ not only for UV light, but also for longer wavelengths [5]. This makes a comparison of $EQE(\sigma_{oc})$ of a passivated to a non-passivated samples of same bulk recombination difficult. If we normalize $EQE(\sigma_{oc})$ to the quantum efficiency at a longer, reference wavelength λ_{ref}, for which $EQE(\sigma_{oc})$ is not affected by surface recombination, measurements of passivated and non-passivated samples can be directly compared:

$$EQE(\sigma_{oc})|_{relative} \equiv \frac{\sigma_{oc}(\lambda)}{N_{ph}(\lambda)} \frac{N_{ph}(\lambda_{ref})}{\sigma_{oc}(\lambda_{ref})} \tag{4}$$

In this case $EQE(\sigma_{oc})|_{relative}$ can be much less than the ideal quantum efficiency at this wavelength. When $EQE(\lambda_{ref})$ is not the maximum quantum efficiency chosen, the $EQE(\sigma_{oc})|_{relative}$ can also surpass the 100 %.

The generation can be described by the fraction of incident photons that are absorbed in the sample, f_{abs}, and the number of incident photons, N_{ph}: $G = f_{abs} \cdot N_{ph}$. If we substitute this into equation (5), we see that we can separate the spectral response of the photoconductance formally into an optical and electrical part, similar to the formulation in equation (3):

$$EQE(\sigma_{oc}) = \frac{\sigma_{oc}(\lambda)}{qN_{ph}(\lambda)} = f_{abs} \cdot \frac{\sigma_{oc}(\lambda)}{qG(\lambda)} \equiv f_{abs} \cdot \eta_c^{oc}(\lambda) \tag{5}$$

As well as for the external quantum efficiency, we can take the relative carrier collection probability, $\eta_c^{oc}(\lambda)|_{relative}$, of two photoconductance measurements:

$$\eta_c^{oc}(\lambda)|_{relative} \equiv \frac{\sigma_{oc}(\lambda)}{G(\lambda)} \frac{G(\lambda_{ref})}{\sigma_{oc}(\lambda_{ref})} \tag{6}$$

This is a generalization of the internal collection probability defined in Ref. [5]. The latter one has been defined only for wavelengths, λ, that are absorbed within the emitter. In contrast, $\eta_c^{oc}(\lambda)|_{relative}$ can be applied to all wavelengths.

3. EXPERIMENTAL

Four *p*-type FZ silicon wafers with thickness 290 µm have been diffused on both sides using a $POCl_3$ source at 860 ºC for 30 min, followed by glass removal and drive-in at 1050 ºC for 60 min. Surface passivation has been achieved by the growth of a thin, invisible (< 20 nm) passivating oxide at 900 ºC for 20 min in O_2 and 10 min in Ar followed by an anneal in forming gas at 400 ºC. These four wafers, labelled A, B, C and D, have essentially the same emitter region and surface passivation conditions. Sample B has been subsequently de-passivated on the front surface, sample C on both surfaces, to investigate the sensitivity of violet response to the surface passivation quality. Their sheet resistance is 42-52 W/sq, which happens to be similar to that of industrial solar cells, although the dopant profile is quite different, with a lower surface concentration and a deeper junction.

A high-efficiency LBSF (Local back surface field) cell has been fabricated at Fraunhofer ISE on 1.25 Ωcm *p*-type FZ silicon with thickness 385 µm with planar surface and double layer (MfF/TiO) antireflection coating. The sheet resistance is 120 Ω/sq, the junction depth is of 2-3 µm under the metal of the front grid and 0.5-1 µm elsewhere [7]. The output parameters are: V_{oc}: 667 mV, I_{sc}: 38.9 mA, η: 20.6 %. After measuring the conventional spectral response, the rear metallization has been etched in hydrochloric acid in order to measure the spectral photoconductance.

A contactless inductively coupled photoconductance apparatus [8] has been used to measure wafer lifetime with the quasi-steady-state technique [9]. Monochromatic illumination between 400 and 1000 nm has been obtained by interposing colour filters between the xenon flash and the wafers. The width of the band passed by the filters was 10-20 nm, the transmission between 20-50 %. After filtering, light intensities above 0.5 suns could be achieved. Heating is still minimal, due to the short duration of the light pulse. The light intensity varies by a factor of 150

within the 12 ms pulse, and this automatically scans the dependence of the photoconductance with injection level. Since recombination is injection-level dependent, it is important to perform the measurements at the different wavelengths in the same excess carrier density within the wafer. A practical way to achieve this is to take the same photoconductance for all wavelengths, because the latter is approximately proportional to the excess carrier density.

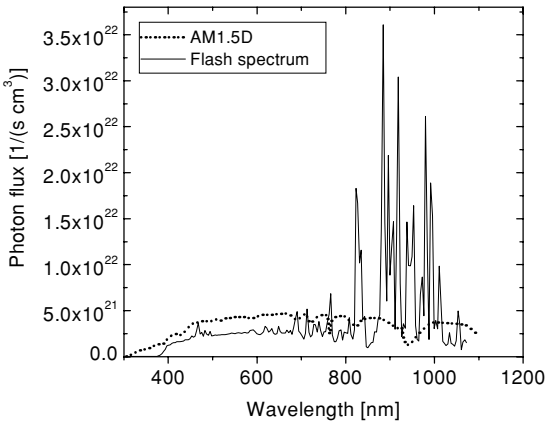

Figure 1: Photon flux of the flash spectrum compared to the AM1.5D spectrum.

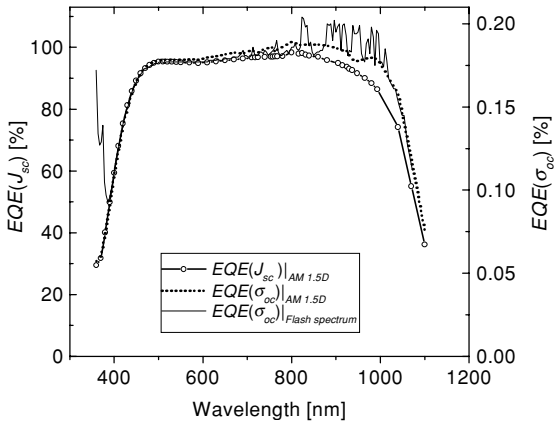

Figure 2: Comparison of the spectral response of short-circuit current of the AM1.5D sun spectrum to the spectral response of the photoconductance of the AM1.5D and the flash spectrum.

The spectrum of the flash and the AM1.5D sun spectrum have been measured with a spectrophotometer. The corresponding photon flux of the spectra shows a similar shape for wavelength 400-800 nm (Figure 1). For higher wavelengths, the flashlight emits high peaks of photon flux, which are significantly different from the solar photon flux. The modelled external quantum-efficiency $EQE(\sigma_{oc})|_{flash\ spectrum}$ of the high-efficiency solar cell further used in this investigation shows the impact of these peaks in the IR (Figure 2). This trend is not seen in the conventional spectral response $EQE(J_{sc})|_{AM1.5D}$ and in the external quantum-efficiency $EQE(\sigma_{oc})|_{AM1.5D}$, when the sun spectrum is used for the simulations (Figure 2). The simulations indicate that, the higher the photon flux, the higher the photoconductance per photon flux. This is due to the injection level dependence of the photoconductance. The impact of the high photon flux in the IR is indeed seen in the photoconductance measurements.

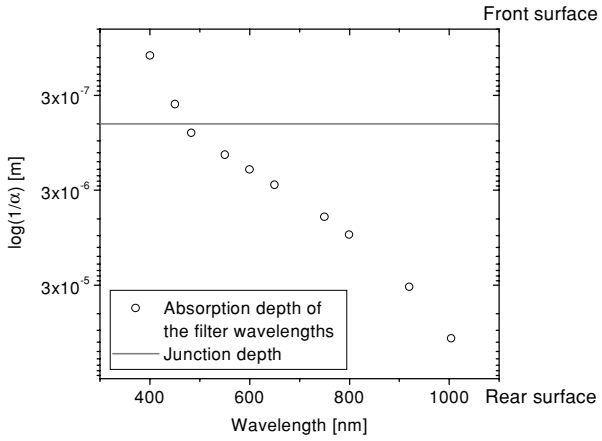

Figure 3: Absorption depth for the wavelength of the different filters used

In Figure 3 absorption depths of the wavelength of the different filters used in the measurements are shown. The absorption depth can be deduced by the absorption coefficient, α, of silicon by $d_{abs} = \log(1/\alpha)$. The scaling of d_{abs} is taken from the front emitter to the rear surface of the samples (thickness: 290 µm). The line indicates the junction depth at 0.6 µm of the emitter devices used in this investigation. The first two filter wavelengths, at 400 and 450 nm, are absorbed in the emitter. Especially for the first filter, the resulting photoconductance will be affected by recombination at the emitter surface. As the diffusion length is very high in the silicon material samples used, the two next filters at 480 and 550 nm are likely to feel the affect of surface recombination, but to a smaller amount.

A spectral calibrated detector has been used to determine the incident photon flux, N_{ph}, after a formula proposed by Bail *et al.* [3]. This photon flux has been corrected to account for the fact that the photoconductance measurement is not strictly steady-state for high lifetimes [10]:

$$N_{ph}(\lambda)|_{corrected} = N_{ph}(\lambda) - W \frac{d\Delta n}{dt} \Big/ f_{abs}(\lambda) \quad (7),$$

while W is the thickness of the wafer and $d\Delta n/dt$ is the derivation of the average excess carrier density. The absorption fraction, f_{abs} has been calculated with PC1D using wavelength dependent reflectance measurements obtained by a spectrophotometer. f_{abs} calculated with PC1D has been compared to the absorption fraction simulated by the ray tracing program SUNRAYS [11] to adjust the internal reflectance at the front and rear silicon surface.

According to our earlier investigation and to the discussion in the introduction, a reference wavelength in the range 700-1000 nm is suitable for passivated high-efficiency emitter devices. For non-passivated high-efficiency emitters wavelengths of 700-800 nm are preferable, because in this region the behaviour of the spectral response of the photoconductance is still similar to the traditional spectral response [5]. As can be seen from the impact of the high photon flux of the flash in the IR, even for passivated high-efficiency solar cell a reference wavelength < 800 nm should be taken. We chose an intermediate reference wavelength of 750 nm. The corresponding absorption depth wavelength is 5.7 µm. Even still close to the junction depth, the photoconductance will not be strongly affected by surface recombination and thus can be taken to compare to the response in the UV.

4. RESULTS AND DISCUSSION

The measured external quantum efficiencies of the open-circuit photoconductance, $EQE(\sigma_{oc})$, of wafers of different emitter diffusions, surface passivation and base resistivities have been compared to PC1D calculations (Figure 4 and 5). Sample A and B have a *n*-type emitter of 50-52 Ω/sq on 1 Ωcm *p*-type silicon; sample C and D an emitter region with sheet resistance 42 Ω/sq on 50 Ωcm *p*-type silicon. The passivating oxide has been etched from the front surface of sample B and from both surfaces of sample C (Table 1). The simulations have been performed with emitter diffusion on the front side. For the rear side, an effective surface recombination velocity (SRV), $S_{eff,rear}$, for the emitter and rear surface recombination has been calculated by PC1D. The spectrum of the flashlight has been used for light excitation. The parameters, which have been changed to match the experimental values, are the front surface recombination velocity, S_{front}, and $S_{eff,rear}$ (Table 1). The measured spectral response of the photoconductance can be well simulated by PC1D (Figure 4 and 5). The resulting S_{front} are 100 cm/s for a passivated surface and 1e7 for a non-passivated surface. These values are typical for a silicon oxide passivated surface and a non-passivated surface, respectively. The spectral response of the photoconductance is very sensitive to surface recombination: If we compare the de-passivated samples B and C to the passivated of the same base resistivity (samples A and D) in Figure 6 and 7, we see that a high surface recombination at the front surface strongly decreases the photoconductance response in the UV. Thus $EQE(\sigma_{oc})$ at λ = 400 nm suffers a recombination loss of ~ 60 %. The removal of the surface passivation does not only affect the UV emitter collection efficiency, but also the overall balance between generation and recombination in the device. The change of $EQE(\sigma_{oc})$ at λ = 920 for example is of ~ 70 %.

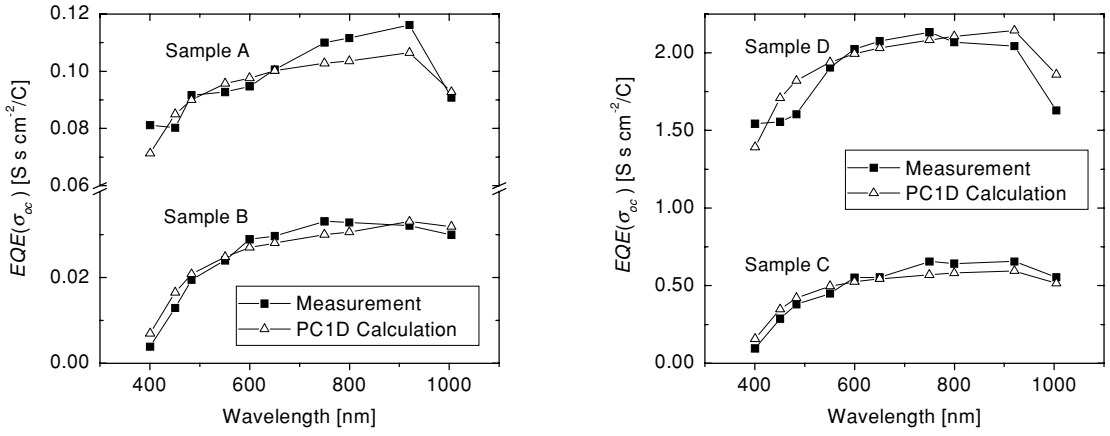

Figure 4 and 5: Comparison of measurement and simulation of the spectral response measurements of the photoconductance of wafers with different phosphorous diffusions, surface passivation conditions.

Table1: Spectral response measurements of the photoconductance for wafers with different phosphorous diffusions, surface passivation conditions and base resistivities compared to PC1D simulations.

Sample	ρ_{bulk} [Ωcm]	Emitter R_{sheet} [Ω/sq]	Surface Passivation	S_{front} (PC1D) [cm/s]	$S_{eff,rear}$ (PC1D) [cm/s]	$EQE(\sigma_{oc})\|_{relative}$ λ=400 nm [%]	$\eta_c^{oc}(\lambda)\|_{relative}$ λ=400 nm [%]	$EQE(\sigma_{oc})\|_{corrected}$ λ=400 nm [%]
A	1	50	Both sides	100	130	73.7	99.5	53.0
B	1	52	Rear side	1e7	110	11.7	16.0	8.3
C	50	42	-	1e7	45	14.5	20.0	9.3
D	50	42	Both sides	100	13	72.4	97.5	46.6

The relative external and internal quantum efficiency of the open-circuit photoconductance, $EQE(\sigma_{oc})|_{relative}$ and $\eta_c^{oc}(\lambda)|_{relative}$, have been calculated, to compare the quantum efficiency of the passivated to the de-passivated samples (Figure 6 and 7). The passivated and de-passivated samples, respectively, show mainly the same wavelengths dependence for both types of devices. In sample B and C, the influence of the front surface recombination leads to far lower values for $\lambda < 600$ nm. The spectral response even decreases towards zero for light absorbed near the front surface. In the range 600-900 nm, $EQE(\sigma_{oc})|_{relative}$ and $\eta_c^{oc}(\lambda)|_{relative}$ only differ slightly. For sample A and D, $\eta_c^{oc}(\lambda)|_{relative}$ is between 90 and 100 % except for λ = 450-500 and 1000 nm. The front surface recombination velocity, S_{front}, calculated with PC1D, corresponds well to $EQE(\sigma_{oc})|_{relative}$ and $\eta_c^{oc}(\lambda)|_{relative}$: for a well passivated surface, $EQE(\sigma_{oc})|_{relative}$ and $\eta_c^{oc}(\lambda)|_{relative}$ are ~ 73 and 98 %, respectively. For a non-passivated surface, the relative quantum efficiencies decrease to 12-15 % and 16-20 %, respectively (Table 1).

The two parameters $EQE(\sigma_{oc})|_{relative}$ and $\eta_c^{oc}(\lambda)|_{relative}$ differ basically in the fact that the external quantum efficiency of the photoconductance, $EQE(\sigma_{oc})$, considers the total number of incident photons onto the wafer, while the internal carrier collection probability, $\eta_c^{oc}(\lambda)$, takes into account only photons, which are absorbed in

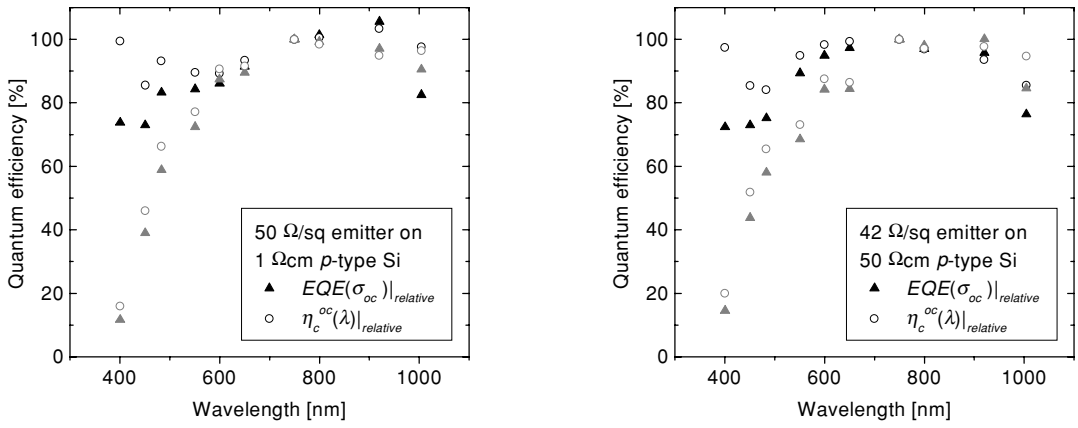

Figure 6 and 7: Comparison of the relative external quantum efficiency to the internal carrier collection probability obtained by photoconductance measurements of wafers with different phosphorous diffusions, surface passivation conditions and base resistivities. The passivated samples A and D are shown with black symbols, the de-passivated samples B and C with grey symbols.

the silicon. The internal parameter, $\eta_c^{oc}(\lambda)$, is only affected by recombination losses, mainly at the emitter and the rear surface. As recombination losses in the bulk are minimal in the high quality float zone silicon used in this investigation, the relative internal carrier collection probability, $\eta_c^{oc}(\lambda)|_{relative}$, is a good measure of recombination losses throughout the device. The external parameter $EQE(\sigma_{oc})$ is also affected by optical losses, i.e. reflection, transmission and absorption losses. The main reflection losses at the Si surface are in the low UV region in the range 300-400 nm and for wavelength > 1000 nm. Transmission occurs for wavelength with absorption depth higher than the wafer thickness. This is the case for high infrared light. Absorption losses are due to the fact that photons with energy lower than the silicon band gap are not absorbed within the wafer. The measurements show

that $\eta_c^{oc}(\lambda)|_{relative}$ can be used in order to deduce absolute recombination losses of silicon solar cell devices.

As can be seen from Figure 7, $EQE(\sigma_{oc})|_{relative}$ can surpass 100 %. This quantum efficiency is representative if we want to evaluate the recombination at the front surface, in comparison to bulk properties. But we will loose the absolute information of the losses, in particular if a high reflection decreases the spectral response throughout the spectrum as in our samples. We propose therefore a correction of $EQE(\sigma_{oc})|_{relative}$, which represents the absolute external quantum efficiency. As the loss of spectral response at the reference wavelength is mainly due to optical losses, reflected by the absorption fraction, f_{abs}, it is convenient to correct the measured spectral response of the photoconductance by this factor:

$$EQE(\sigma_{oc})\big|_{corrected} \equiv f_{abs}(\lambda_{ref}) \cdot EQE(\sigma_{oc})\,|_{relative} \tag{8}$$

This corrected spectral response has been compared with the conventional external quantum efficiency $EQE(J_{sc})$ calculated by PC1D for the sample A-D (Figure 8 and 9). The same details as above have been used for the simulation. The correction shifts the spectral response to lower values < 80 %. A good agreement between measurement of photoconductance and simulation of short-circuit current can be found.

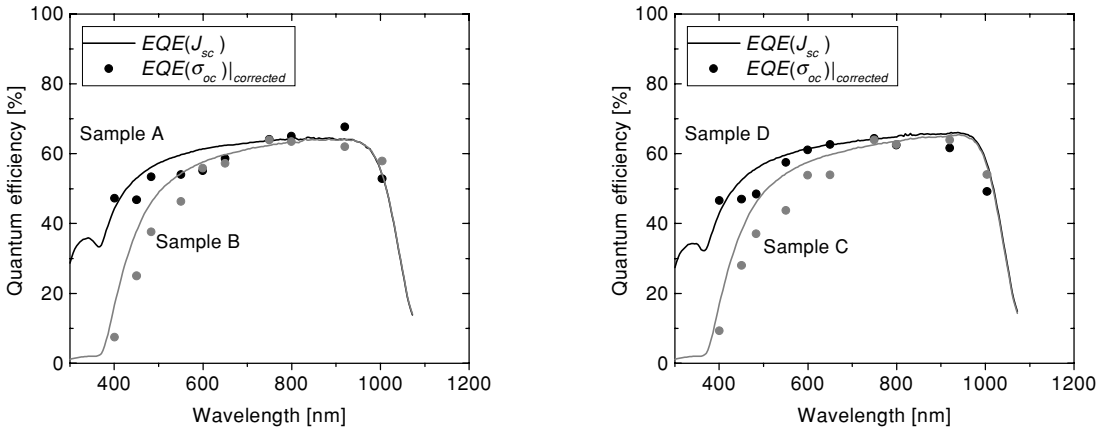

Figure 8 and 9: Comparison of the conventional spectral response method to the scaled new spectral response technique of wafers with different phosphorous diffusions, surface passivation conditions and base resistivities compared to PC1D simulations.

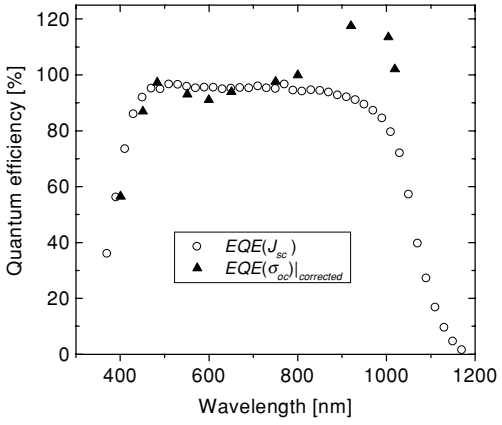

Figure 10: Absorption depth for the wavelength of the different filters used

The corrected external quantum efficiency of the open-circuit photoconductance, $EQE(\sigma_{oc})|_{corrected}$, has been compared to the traditional external quantum-efficiency, $EQE(J_{sc})$ for a high-efficiency PERC cell with 120 Ω/sq emitter on 1.25 Ωcm p-type FZ-silicon (Figure 10). First the IV characteristics and the traditional spectral response has been measured. Then the rear metallization has been removed and the measurement of the spectral response of the photoconductance has been performed.

The comparison of $EQE(\sigma_{oc})|_{corrected}$ and $EQE(J_{sc})$ shows that a good agreement can be found for all wavelengths except in the IR. The divergence in the infrared is due to the higher sensitivity of the spectral photoconductance to charge carriers generated deep in the wafer and to the high photon flux peaks in the IR of the flashlight. Both trends are not seen in the short-circuit response. Furthermore a very good agreement between experiment and theory can be found for both.

5. CONCLUSION

We have analyzed the spectral response of the open-circuit photoconductance of silicon solar cell precursors and of a high-efficiency solar cell. Definitions of the external and internal quantum efficiency of the photoconductance, $EQE(\sigma_{oc})$ and $\eta_c^{oc}(\lambda)$, have been derived. A motivation and a formula for a correction of the relative external quantum efficiency have been given, which will provide a measure of absolute efficiency losses. $\eta_c^{oc}(\lambda)|_{relative}$, as well as the scaled external quantum efficiency of the photoconductance, $EQE(\sigma_{oc})|_{corrected}$, are suitable to characterize efficiency losses for wavelength < 800 nm. PC1D simulations of the measurements have been performed, which indicate a good agreement between experiment and simulation. The comparison of the conventional spectral response method and the QSSPC-λ technique on a high-efficiency cell demonstrates a validation of the latter. As there is great interest in the characterization of the emitter region and in particular directly after junction formation, the QSSPC-λ method can be seen as a valuable alternative to the conventional spectral response technique. The QSSPC-λ technique has the great advantage over the conventional spectral response that it can also be used with solar cell precursors, that is, not requiring metal contacts and complex processing.

6. ACKNOWLEDGMENTS

H.Mäckel is supported by the German scholarship program of the Deutsche Akademische Austauschdienst.

7. REFERENCES

[1] A. Cuevas, R. A. Sinton and M. Stuckings (1996), *Determination of recombination parameters in semiconductors from photoconductance measurements, Proceedings of the 1996 Conference on Optoelectronic and Microelectronic Materials and Devices*, Canberra, ACT, Australia, 8-11 Dec., 1996, pp. 16-19.
[2] R. Brendel (1995), *Note on the interpretation of injection level dependent surface recombination velocities,* Applied Physics A, 60, 523.
[3] M. Bail and R. Brendel (2000), *Separation of bulk and surface recombination by steady state photoconductance measurements, 16th European Photovoltaic Solar energy Conversion*, Glasgow, UK, 1-5 May, 2000, pp. 98.
[4] A. Cuevas, M. Kerr, D. Macdonald and R. A. Sinton (2000), *Emitter quantum efficiency from contactless photoconductance measurements, Proceedings of 28th IEEE Photovoltaic Specialists Conference*, Anchorage, AK, USA, 15-22 Sept, 2000.
[5] A. Cuevas, R. A. Sinton, M. Kerr, D. Macdonald and H. Mäckel (2001), *A contactless photoconductance technique to evaluate the quantum efficiency of solar cell emitters,* in press in Solar Energy Material and Solar Cells.
[6] P. Campbell, M. Keevers and B. Vogl (2001), *Characterisation of light trapping in silicon films by spectral photoconductance measurements,* Solar Energy Materials & Solar Cells, 66 (1-4), 187-193.
[7] A. Goetzberger, B. Voß and J. Knobloch (1994), *Sonnenenergie: Photovoltaik*, Teubner Studienbücher Physik, Stuttgart.
[8] G. C. Sinton Consulting, Boulder, CO 80305.
[9] R. A. Sinton and A. Cuevas (1996), *Contactless determination of current-voltage characteristics and minority-carrier lifetimes in semiconductors from quasi- steady-state photoconductance data,* Applied Physics Letters, 69 (17), 2510-2512.
[10] H. Nagel, C. Berge and A. G. Aberle (1999), *Generalized analysis of quasi-steady-state and quasi-transient measurements of carrier lifetimes in semiconductors,* Journal of Applied Physics, 86 (11), 6218-6221.
[11] R. Brendel (1993), *Simple prism pyramids: a new light trapping texture for silicon solar cells, Proceedings of the 23rd IEEE Photovoltaic Specialists Conference*, Louisville, Kentucky, USA, 10-14 May, 1993, pp. 1490, 1252-1495.